Simulation of X-ray diffraction-line broadening due to dislocations in a model composite material

Bor, T.C.; Cleveringa, H.H.M.; Delhez, R.; van der Giessen, E.

Published in:
Materials science and engineering a-Structural materials properties microstructure and processing

DOI:
10.1016/S0921-5093(00)01648-8

Publication date:
2001

ELSEVIER

Materials Science and Engineering A309–310 (2001) 505–509

MATERIALS SCIENCE & ENGINEERING A

www.elsevier.com/locate/msea

Simulation of X-ray diffraction-line broadening due to dislocations in a model composite material

T.C. Bor [a,b], H.H.M. Cleveringa [b], R. Delhez [a,*], E. Van der Giessen [b]

[a] *Laboratory of Materials Science, Rotterdamseweg 137, 2628 AL Delft, The Netherlands*
[b] *Koiter Institute Delfi, Deift Universiy of Technology, Mekelweg 2, 2628 CD Delft, The Netherlands*

Abstract

X-ray diffraction-line profiles of two-dimensional, plastically deformed model composite materials are calculated and analysed in detail. The composite consists of elastic reinforcements in a crystalline solid and is subjected to macroscopic shear. Slip occurs in the matrix only due to the collective motion of discrete dislocations on a single set of parallel slip planes. The results of dislocation dynamics computations are used as input for the calculation of the line profiles. The line profiles are computed directly using the kinematics approach, without making a priori assumptions on the dislocation distributions. Two steps are required. First, the full intensity distribution of a single crystal of composite material is calculated. Then, assuming a perfectly random orientation distribution of such single crystals, powder diffraction-line profiles are determined. Results will be presented for several orders of reflection and in different crystallographic directions. The broadening of the line profiles is shown to be not only determined by the density of dislocations, but also by their spatial distribution.

Keywords: Simulation of X-ray diffraction; Model composite; Discrete dislocation plasticity

1. Introduction

Plastic deformation in the matrix of composite materials is hindered by the presence of elastic reinforcements. As slip of dislocations on glide planes blocked by reinforcements is often hindered or retarded, specific patterns in the distribution of dislocations are formed, such as the piling-up of dislocations on the sides of the reinforcements. These dislocations are geometrically necessary for the composite material to comply with the applied deformation [1].

Several experimental techniques exist which enable a study of deformed materials containing dislocations, of which X-ray diffraction (XRD) is an important one. XRD line profiles are broadened due to strain fields which, in part, are associated with the presence of dislocations. The broadening depends on the reflection and the type and orientation of the dislocations. The analysis of the broadening of these line profiles is not straightforward [2]. A model of the spatial and orientational distribution of dislocations must be used to predict the line profile shape and width. Examples of such models using idealized dislocation distributions are those proposed by Wilkens [3], Groma et al., [4] and Groma [5], which involve more or less random distributions of dislocations. Evidently, these model descriptions cannot be applied if specific, non-random, patterns occur in the dislocation distribution.

In this work we propose a different route of analysis, which is not based on presumed dislocation distributions. Instead, the deformation of a model composite material is simulated with the aid of a recently developed simulation method to obtain a physically realistic dislocation distribution [6,7]. Subsequently, XRD line profiles of the model composite material are calculated and interpreted. A similar procedure for small angle scattering has been conducted in [8].

2. Theory

2.1. Model composite

An infinitely large two-dimensional single crystalline material is analysed that contains elastic reinforcements in a matrix [6,7]. The reinforcements are arranged in a doubly periodic hexagonal array as shown in Fig. 1. The unit cell describing the particle arrangement is defined by $\boldsymbol{a}_1$ and $\boldsymbol{a}_2$ with $a_2 = 2\,\mu\text{m}$ and $a_1/a_2 = \sqrt{3}$ in the undeformed state. It contains two reinforcements of size $2w_f \times 2h_f$ with one located in the center of the unit cell. Here, we consider the case with an area fraction of particles of 20%, with an aspect ratio $h_f/w_f = 2$.

* Corresponding author. Tel.: +31-15-2782261; fax: +31-15-2786730.
E-mail address: d.delhez@tnw.tudelft.nl (R. Delhez).

0921-5093/01/$ – see front matter
PII: S0921-5093(00)01648-8

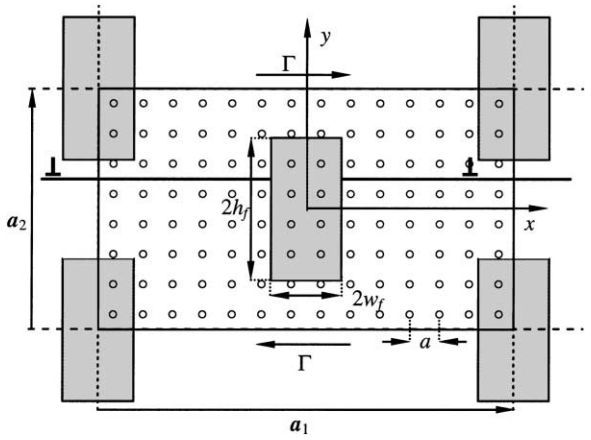

Fig. 1. Unit cell of composite material with a doubly-periodic array of elastic particles (particle dimensions $2h_f \times 2w_f$ with $h_f/w_f = 2$ and area fraction 20%) defined by $\boldsymbol{a}_1$ and $\boldsymbol{a}_2$, with $a_1 = \sqrt{3}a_2$ and $a_2 = 2\,\mu\text{m}$. All slip planes are taken to be parallel to the applied shear direction with Γ the magnitude of the shear. The unit cell contains an array of $2N_1 \times 2N_2 = 14 \times 8$ atoms with a, the atomic distance.

The unit cell is subjected to plane strain simple shear in the x-direction and periodic boundary conditions are imposed along the lateral sides $x = \pm a_1/2$. All slip planes are blocked by impenetrable reinforcements, so that the central reinforcement must rotate to accommodate the shear and (geometrically necessary) dislocations pile up against the reinforcement sides.

2.2. Discrete dislocation plasticity

In the discrete dislocation description of plasticity in the matrix, the dislocations are represented as line defects in a linear elastic continuum [6,7]. Only edge dislocations on a single slip system are considered for the present model composite. The glide direction is in the x-direction, the slip plane normal is in the y-direction and all dislocations have the same Burgers vector magnitude, $b = 0.5\,\text{nm}$. The latter requires the solution of the boundary value problem which is done by decomposing the fields as the superposition of two fields: (i) the sum of the fields of the individual dislocations in their present configuration but in an infinite medium of the homogeneous matrix material, and (ii) the image field that corrects for the tractions and displacements on the boundary of the unit cell and that imposes the boundary conditions. The second field is smooth and can be conveniently calculated by the finite element method. The deformation history is calculated in an incremental manner. For each time increment the following steps are required: (i) determination of the Peach–Koehler forces on the dislocations, (ii) determination of the changes in the dislocation structure, and (iii) determination of the stress and strain state for the adjusted dislocation arrangement.

Initially no dislocations are present. On each slip plane a distribution of two-dimensional Frank–Read sources is specified. Each source generates a dislocation dipole under certain conditions. Dislocation motion is assumed to occur only by glide on the glide planes; no cross slip is assumed. The dislocation velocity is taken proportional to the respective Peach–Koehler forces. Annihilation of opposite signed dislocations occurs when they come within a critical distance. Further details are described in [6,7].

2.3. X-ray diffraction

In order to calculate X-ray diffraction-line profiles the unit cell is filled with a two-dimensional array of $2N_1 \times 2N_2$ atoms divided over matrix and reinforcements as schematically indicated in Fig. 1. The displacement field is sampled at the original reference positions of the atoms rendering the displacement of the atoms from their reference positions. Ideally the atomic distance should equal the magnitude of the Burgers vector $\boldsymbol{b}$. However, the very large number of atoms required in such cases poses computational problems. Fortunately, the information of the displacement fields that is relevant to the shape and width of powder diffraction-line profiles can also be obtained by employing a larger sampling distance. However, in order to obtain a reflection corresponding to the original atomic distance ($a = b$), the order of reflection should be increased by the same amount. In this case a factor of eight is used which corresponds to a conveniently sized two-dimensional array of 866×500 atoms.

According to the kinematical theory of diffraction, the (hk) intensity distribution of a single (here two-dimensional) crystal in reciprocal space is given by the square of the modulus of the product of the structure factor F and the crystal factor G [9]. The structure factor F for the (hk) reflection of a unit cell is given by, neglecting second order effects, $F = \sum_n f_n \mathrm{e}^{2\pi \mathrm{i}(\boldsymbol{H}_{\mathrm{B}}^{hk}\boldsymbol{u}_n)} \mathrm{e}^{2\pi \mathrm{i}(\boldsymbol{H}\boldsymbol{r}_n^0)}$ with f_n the atomic scattering factor of atom n at position $\boldsymbol{r}_n = \boldsymbol{r}_n^0 + \boldsymbol{u}_n$ in the unit cell with $\boldsymbol{r}_n^0$ the position of atom n in the undeformed state and $\boldsymbol{u}_n$ the displacement of atom n from its strain-free location due to the presence of dislocations and image fields. Furthermore, $\boldsymbol{H} = h\boldsymbol{b}_1 + k\boldsymbol{b}_2$ denotes the diffraction vector, where $\boldsymbol{b}_1$ and $\boldsymbol{b}_2$ denote the axes of the unit cell of the corresponding reciprocal lattice and $\boldsymbol{H}_{\mathrm{B}}^{hk}$ denotes the (hk) Bragg reflection for the lattice spacings of the (shear) deformed unit cell. It can be shown for an infinitely large single crystal composed of identical unit cells that the crystal factor G equals non-zero only for specific values of h and k; the intensity distribution in reciprocal space thus consists of a collection of line intensities instead of a continuous distribution of intensity. In this work, the (hk) reflections are indicated with respect to vectors $\boldsymbol{a}_1/2N_1$ and $\boldsymbol{a}_2/2N_2$, which characterize the average atomic distances along the sides of the unit cell [9].

From the (two-dimensional) intensity distribution in reciprocal space of an (hk) reflection, an $\{hk\}$ powder diffraction-line profile is constructed in the following way.

A powder is considered which consists of an infinite number of identical single crystals as the one considered

above and with a perfectly random distribution of such single crystals. Then, the intensity distribution of the powder is obtained from the intensity distribution in reciprocal space for the single crystal through integration in reciprocal space along a line perpendicular to the diffraction vector of the (hk) Bragg reflection at a specified length of the diffraction vector $|\boldsymbol{H}|$. The full $\{hk\}$ powder diffraction-line profile is then obtained by repeating this procedure for an appropriate range of diffraction vector lengths [9]. Since the spacing between the line intensities of such line profiles is often irregular, the line profiles are converted into histograms of constant spacing; they are presented by continuous lines through the data points.

3. Results and discussion

The simulated distribution of dislocations within the unit cell, for a shear $\Gamma = 1\%$, is presented in Fig. 2a. Powder diffraction-line profiles of the type $\{0h\}$, $\{hh\}$ and $\{h0\}$, respectively, are shown for three orders of reflection in Fig. 2b–d. They represent line profiles with the diffraction vector mainly in the [0 1], [1 1] and [1 0] direction, respectively. Only the atoms in the matrix contribute to the diffraction process: $f_n = 1$; for the atoms within the particles: $f_n = 0$. The powder diffraction-line profiles are broadened due to the strain field in the unit cell ("strain" broadening) and due to finite distances in the matrix between the particles ("size" broadening) [9,10]. Since the broadening

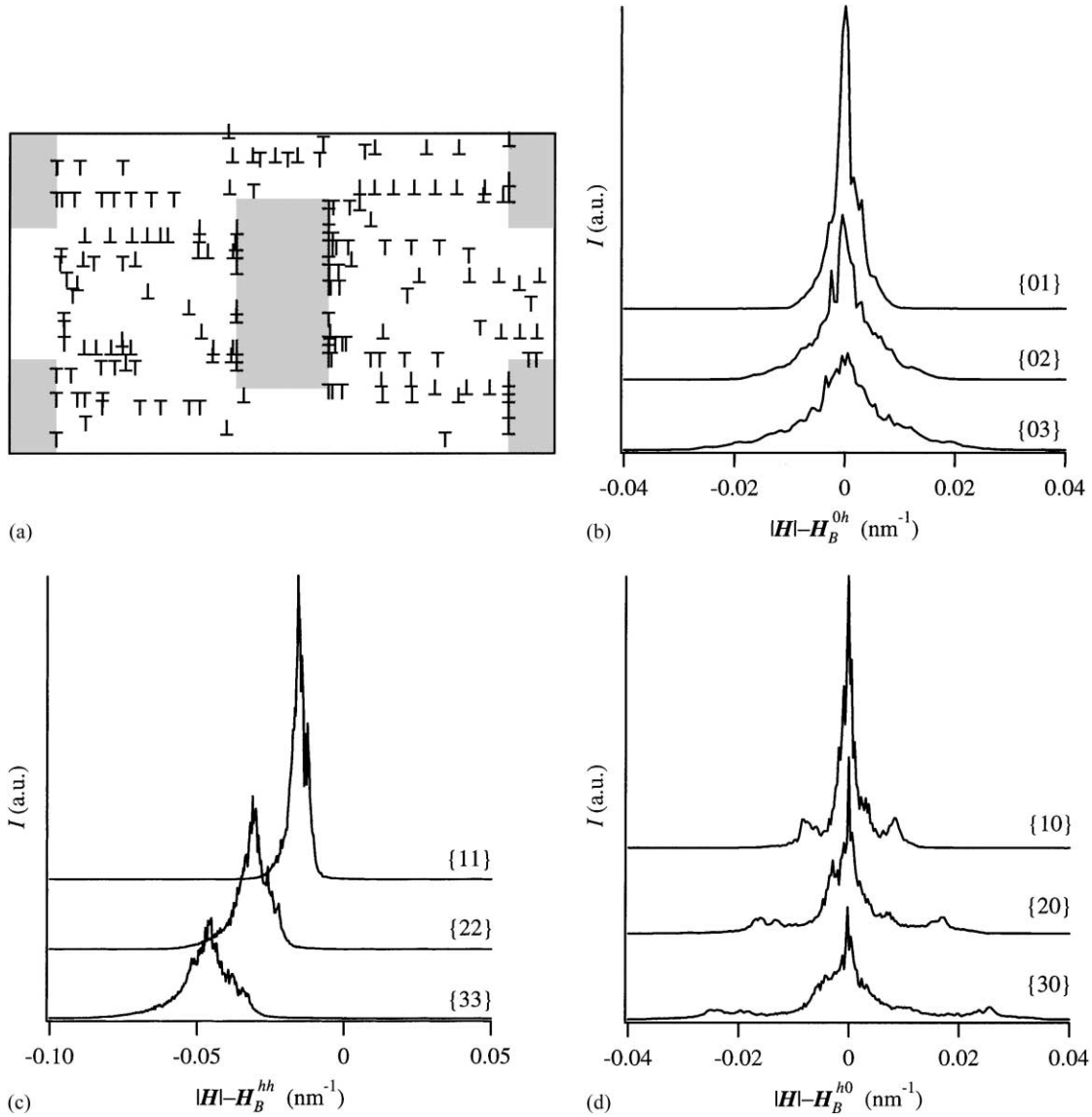

Fig. 2. (a) Distribution of dislocations at $\Gamma = 1\%$; (b)–(d). Corresponding powder diffraction-line profiles for three orders of reflection of type $\{0h\}$, $\{hh\}$ and $\{h0\}$. The unit cell is sampled with an array of $2N_1 \times 2N_2 = 866 \times 500$ atoms. All reflections correspond to an atomic distance, a, equal to the magnitude of the Burgers vector, $a = b = 0.5$ nm. The origins of the abscissae are taken at the location of the respective Bragg reflections in reciprocal space corresponding to the deformed unit cell.

exhibits a strong dependence on the order of reflection, the broadening is mostly due to "strain" [2,9]; the contribution of the "size" broadening is very small here. From Fig. 2b–d it becomes clear that the shape and width of the powder diffraction-line profiles are strongly direction dependent. The $\{0h\}$ reflections are more or less symmetric, the $\{hh\}$ reflections are asymmetric and shifted and the slightly asymmetric $\{h0\}$ reflections contain additional peaks on either side of the main peak near $|H| - H_B^{10} = \pm 0.008\,\mathrm{nm}^{-1}$. The remaining of this work concentrates on the side peaks through a study of some idealized dislocation structures.

Three types of idealized dislocation distributions were deduced from Fig. 2a with the number of dislocations comparable with the discrete dislocation simulation case: (I) dislocations distributed at random in the matrix, (II) dislocations piled up against the sides of the reinforcements (geometrically necessary dislocations), and (III) strings of dislocations on glide planes inbetween one of the edge reinforcements and the central reinforcement. For distribution (I)160 dislocations were distributed on the glide planes, an equal amount of both signs; distributions (II) and (III) are displayed in Fig. 3. For these idealized distributions, only the dislocation fields are used, which implies no elastic shear applied onto the sides of the unit cell. Therefore, the $\{10\}$ line profile of the discrete dislocation simulation (see Fig. 2d) is recalculated considering only the contribution of the dislocations to the displacement field within the unit cell (see Section 2.2). All $\{10\}$ powder diffraction-line profiles are displayed in Fig. 4.

The exclusion of the contribution of the image fields from the discrete dislocation simulation has a large effect on the position of the side peaks: without this contribution the matrix is strained less (elastically) and therefore the peaks are located closer to the main peak at $|H| - H_B^{10} = \pm 0.005\,\mathrm{nm}^{-1}$, as also indicated by the arrows. Each type of idealized dislocation distribution has a different effect on the shape of the corresponding $\{10\}$ line profile. The randomly distributed dislocations cause a more or less

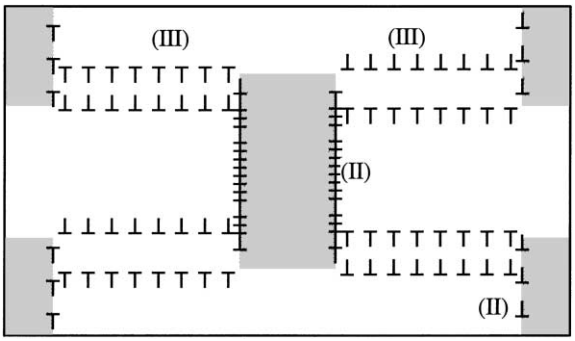

Fig. 3. Some idealized dislocation structures deduced from the result of the discrete dislocation simulation in Fig. 2a: (II) dislocations piled up against the sides of the reinforcements, and (III) strings of dislocations on glide planes inbetween one of the edge reinforcements and the central reinforcement.

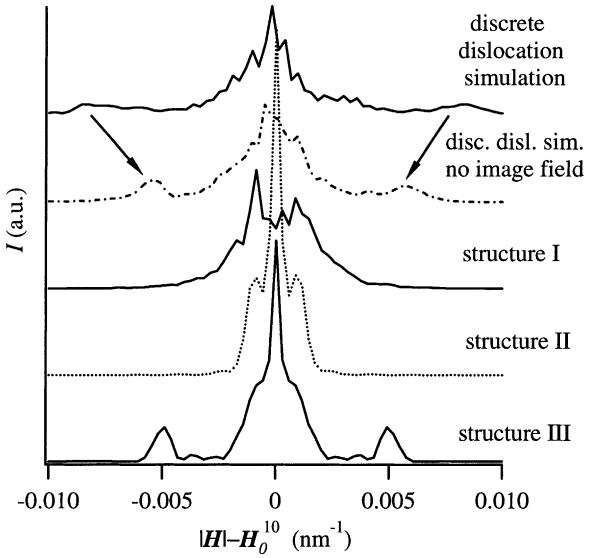

Fig. 4. $\{10\}$ Powder diffraction-line profiles of a unit cell containing the dislocation distribution according to the discrete dislocation simulation (see Fig. 2a) with and without the contribution of image fields; $\{10\}$ Powder diffraction-line profiles of a unit cell containing an idealized dislocation distribution: (I) random distribution of dislocations in the matrix, (II) dislocations piled up against the sides of the reinforcements, and (III) strings of dislocations on glide planes inbetween one of the edge reinforcements and the central reinforcement (see also Fig. 3).

symmetric $\{10\}$ line profile with a broadening of comparable magnitude as the $\{10\}$ line profile of the discrete dislocation simulation ($\{10\}_{\mathrm{dis}}$). No side peaks are observed. The dislocations piled-up along the sides of the reinforcements cause small side peaks very near the main peak (at $|H| - H_B^{10} = \pm 0.001\,\mathrm{nm}^{-1}$), but these cannot be ascribed to the side peaks in $\{10\}_{\mathrm{dis}}$. The parallel strings of dislocations do cause side peaks at approximately the same $|H| - H_B^{10}$-values as in case of $\{10\}_{\mathrm{dis}}$.

These side peaks can be explained as follows. The parallel strings of dislocations cause an average strain in the [1 0] direction within the region they enclose, with a sign depending on the orientation of the dislocations. The regions are aligned parallel to the [1 0] direction and encompass the matrix part of the unit cell in this direction.

According to diffraction theory [9], columns of atoms parallel to the diffraction vector diffract separately (incoherently) from one another. Therefore, the more or less homogeneously strained regions diffract separately from the remaining part of the matrix and this causes side peaks to appear on either side of the main peak. These are displaced from the location of the main peak with a shift proportional to the average strain in the [1 0] direction in the regions.

4. Conclusions

Plastic deformation of a composite material, consisting of a matrix with impenetrable reinforcements that block the

slip planes in the matrix, leads to distinct dislocation distributions. Analysis of X-ray diffraction-line profiles, calculated of the deformed composite materials, shows that different types of dislocation distributions give rise to different changes of the line profiles. This holds the promise of XRD broadening being capable of assessing dislocation structures. Further work is needed to assess if and how this can be performed on real XRD data.

References

[1] M.F. Ashby, Phil. Mag. 21 (1970) 399.
[2] R. Delhez, Th.H de Keijser, E.J. Mittemeijer, Fresenius Z. Anal. Chem. 312 (1982) 1.
[3] M. Wilkens, Acta Metall. 17 (1969) 1155.
[4] I. Groma, T. Ungar, M. Wilkens, J. Appl. Cryst. 21 (1988) 47.
[5] I. Groma, Phys. Rev. B 57 (1998) 7535.
[6] E. Van der Giessen, A. Needleman, Model. Simul. Mater. Sci. Eng. 3 (1995) 689.
[7] H.H.M. Cleveringa, E. Van der Giessen, A. Needleman, Acta Mater. 45 (1997) 3163.
[8] V.B. Shenoy, H.H.M. Cleveringa, R. Philips, E. Van der Giessen, A. Needleman, Model. Simul. Mater. Sci. Eng. 8 (2000) 557.
[9] B.E. Warren, X-ray Diffraction, Reading, Addison–Wesley, Massachusetts, 1969.
[10] T.C. Bor, R. Delhez, E.J. Mittemeijer, E. Van der Giessen, J. Appl. Phys., submitted.